

High-Resolution Spectrum-Estimation Methods for Signal Analysis in Power Systems

Tadeusz Lobos, Zbigniew Leonowicz, *Member, IEEE*, Jacek Rezmer, and Peter Schegner, *Member, IEEE*

Abstract—The spectrum-estimation methods based on the Fourier transform suffer from the major problem of resolution. The methods were developed and are mostly applied for periodic signals under the assumption that only harmonics are present and the periodicity intervals are fixed, while periodicity intervals in the presence of interharmonics are variable and very long. A novel approach to harmonic and interharmonic analysis based on the “subspace” methods is proposed. Min-norm and music harmonic retrieval methods are examples of high-resolution eigenstructure-based methods. Their resolution is theoretically independent of the signal-to-noise ratio (SNR). The Prony method as applied for parameter estimation of signal components was also tested in the paper. Both the high-resolution methods do not show the disadvantages of the traditional tools and allow exact estimation of the interharmonic frequencies. To investigate the methods, several experiments were carried out using simulated signals, current waveforms at the output of an industrial frequency converter, and current waveforms during out-of-step operation of a synchronous generator. For comparison, similar experiments were repeated using the fast Fourier transform (FFT). The comparison proved the superiority of the new methods.

Index Terms—Eigenvalues and eigenfunctions, harmonic analysis, industrial power-system harmonics, inverters, signal resolution, synchronous-generator transient analysis, time-frequency analysis.

I. INTRODUCTION

TODAY, the quality of voltage waveforms is an issue of utmost importance for power utilities, electric energy consumers, and also for manufacturers of electric and electronic equipment. The liberalization of energy markets will strengthen the competition and is expected to drive down the energy prices. This is the reason for the requirements concerning the power quality. The voltage waveform is expected to be a pure sinusoidal with a given frequency and amplitude. Modern frequency power converters generate a wide spectrum of harmonic components that determine the quality of the delivered energy and increase the energy losses as well as decrease the reliability of a power system. In some cases, large converter systems generate not only characteristic harmonics typical for the ideal converter operation but also a considerable amount of noncharacteristic

harmonics and interharmonics, which may strongly determine the quality of the power-supply voltage [1], [2]. The estimation of the components is very important for control and protection tasks.

There are many different approaches for measuring harmonics like fast Fourier transform (FFT), application of adaptive filters, artificial neural networks, singular value decomposition (SVD), higher order spectra, etc. [3]–[7]. Most of these approaches operate adequately only in the narrow range of frequencies and at moderate noise levels. Estimation of the power spectral density (PSD) or simply the spectrum of discretely sampled deterministic and stochastic processes is usually based on procedures employing the FFT. The most often-used spectral-estimation techniques are the following:

- 1) indirect approach via an autocorrelation estimate (Blackman–Tukey);
- 2) direct approach via FFT operation (periodogram);
- 3) modified averaged periodogram (Welch).

The conventional FFT spectral estimation is based on a Fourier-series model of the data, that is, the process is assumed to be composed of a set of harmonically related sinusoids. This approach to spectrum analysis is computationally efficient and produces reasonable results for a large class of signal processes. In spite of these advantages, there are several inherent performance limitations of the FFT approach. The most prominent limitation is that of frequency resolution, i.e., the ability to distinguish the spectral responses of two or more signals. Because of some invalid assumptions (zero data or repetitive data outside the duration of observation) made in this method, the estimated spectrum can be a smeared version of the true spectrum [8].

A second limitation is due to noncoherent signal sampling of the data, which manifests itself as a leakage in the spectral domain—energy in the main lobe of a spectral response leaks into the side lobes, obscuring and distorting other spectral responses that are present. Windowing is used to reduce the leakage, but it introduces additional distortions.

These two performance limitations of the FFT approach are particularly troublesome when analyzing short data records. Short data records occur frequently in practice because many measured processes are brief in duration or have slowly time-varying spectra, which can be considered constant only for short record lengths. These methods usually assume that only harmonics are present and the periodicity intervals are fixed, while periodicity intervals in the presence of interharmonics are variable and very long [1].

Manuscript received September 6, 2004; revised October 3, 2005. This work was supported in part by the Deutsche Forschungsgemeinschaft (DFG), Germany, and in part by the State Committee for Scientific Research (KBN), Poland.

T. Lobos, Z. Leonowicz, and J. Rezmer are with the Department of Electrical Engineering, Wrocław University of Technology, Wrocław 50-370, Poland.

P. Schegner is with the Institute of Electrical Power Systems and High Voltage Engineering, Dresden University of Technology, Dresden D-01062, Germany.

Digital Object Identifier 10.1109/TIM.2006.862015

90 The Prony method is a technique for modeling sampled data
 91 as a linear combination of exponentials. Although it is not a
 92 spectral-estimation technique, the Prony method has a close re-
 93 lationship to the least squares linear prediction algorithms used
 94 for autoregressive (AR) and autoregressive-moving-average
 95 (ARMA) parameter estimation. The Prony method seeks to fit
 96 a deterministic exponential model to the data in contrast to AR
 97 and ARMA methods that seek to fit a random model to the
 98 second-order data statistics. In [9], a new method of real-time
 99 measurement of power-system frequency based on the Prony
 100 model is presented.

101 The most recent methods of spectrum estimation are based
 102 on the linear algebraic concepts of subspaces and have been
 103 called “subspace methods” [10]. Its resolution is theoretically
 104 independent of the signal-to-noise ratio (SNR). The model
 105 of the signal in this case is a sum of random sinusoids in
 106 the background of a noise of a known covariance function.
 107 Pisarenko first observed that the zeros of the z transform of
 108 the eigenvector, corresponding to the minimum eigenvalue of
 109 the covariance matrix, lie on the unit circle and their angular
 110 positions correspond to the frequencies of the sinusoids. In a
 111 later development, it was shown that the eigenvectors might
 112 be divided into two groups, namely, the eigenvectors spanning
 113 the signal space and the eigenvectors spanning the orthogonal
 114 noise space. The eigenvectors spanning the noise space have
 115 eigenvalues that are the smallest and that equal to the noise
 116 power. One of the most important techniques, based on the
 117 Pisarenko approach of separating the data into signal and noise
 118 subspaces, is the min-norm method.

119 To investigate the ability of the methods, several experiments
 120 were performed. Simulated signals and current waveforms at
 121 the output of an industrial frequency converter as well as current
 122 waveforms during out-of-step operation of a synchronous gen-
 123 erator were investigated. For comparison, similar experiments
 124 were repeated using the FFT.

125 In this paper, the frequencies of signal components are esti-
 126 mated using the Prony model and the min-norm subspace
 127 method.

128 In other publications, the authors investigated different as-
 129 pects of signal analysis in power systems. In [11], the main part
 130 was devoted to the investigation of the frequency converter with
 131 emphasis to real signals, whereas in [12], only some cases of
 132 simulated industrial frequency converters were reported. This
 133 paper presents the case of out-of-step operation of synchronous
 134 generators, the analysis of waveforms from the power supply
 135 of dc arc furnaces, and the detailed analysis of frequency
 136 converters as examples of analysis using the Prony and min-
 137 norm methods in power systems.

138 II. PRONY METHOD

139 Assuming the N complex data samples $x[1], \dots, x[N]$; the
 140 investigated function can be approximated by M exponential
 141 functions

$$y[n] = \sum_{k=1}^M A_k e^{(\alpha_k + j\omega_k)(n-1)T_p + j\psi_k} \quad (1)$$

where $n = 1, 2, \dots, N$; T_p is the sampling period; A_k is the
 142 amplitude; α_k is the damping factor; ω_k is the angular velocity;
 143 and ψ_k is the initial phase. 144

The discrete-time function may be concisely expressed in
 145 the form 146

$$y[n] = \sum_{k=1}^M \mathbf{h}_k \mathbf{z}_k^{n-1} \quad (2)$$

where 147

$$\mathbf{h}_k = A_k e^{j\psi_k}, \quad \mathbf{z}_k = e^{(\alpha_k + j\omega_k)T_p}.$$

The estimation problem is based on the minimization of the
 148 squared error over the N data values 149

$$\delta = \sum_{n=1}^N |\varepsilon[n]|^2 \quad (3)$$

where 150

$$\varepsilon[n] = x[n] - y[n] = x[n] - \sum_{k=1}^M \mathbf{h}_k \mathbf{z}_k^{n-1}. \quad (4)$$

This turns out to be a difficult nonlinear problem. It can
 151 be solved using the Prony method that utilizes linear-equation
 152 solutions. If as many data samples are used as there are expo-
 153 nential parameters, then an exact exponential fit to the data may
 154 be made. 155

Consider the M -exponent discrete-time function 156

$$x[n] = \sum_{k=1}^M \mathbf{h}_k \mathbf{z}_k^{n-1}. \quad (5)$$

The M equations of (5) may be expressed in matrix from as 157

$$\begin{bmatrix} \mathbf{z}_1^0 & \mathbf{z}_2^0 & \cdots & \mathbf{z}_M^0 \\ \mathbf{z}_1^1 & \mathbf{z}_2^1 & \cdots & \mathbf{z}_M^1 \\ \vdots & \vdots & \ddots & \vdots \\ \mathbf{z}_1^{M-1} & \mathbf{z}_2^{M-1} & \cdots & \mathbf{z}_M^{M-1} \end{bmatrix} \cdot \begin{bmatrix} \mathbf{h}_1 \\ \mathbf{h}_2 \\ \vdots \\ \mathbf{h}_M \end{bmatrix} = \begin{bmatrix} x[1] \\ x[2] \\ \vdots \\ x[M] \end{bmatrix}. \quad (6)$$

The matrix equation represents a set of linear equations that
 158 can be solved for the unknown vector of amplitudes. Prony
 159 proposed to define the polynomial that has the \mathbf{z}_k exponents
 160 as its roots 161

$$F(\mathbf{z}) = \prod_{k=1}^M (\mathbf{z} - \mathbf{z}_k) = (\mathbf{z} - \mathbf{z}_1) \cdot (\mathbf{z} - \mathbf{z}_2) \cdot (\cdots) \cdot (\mathbf{z} - \mathbf{z}_M). \quad (7)$$

The polynomial may be represented as the sum 162

$$F(\mathbf{z}) = \sum_{m=0}^M a[m] \mathbf{z}^{M-m} = a[0] \mathbf{z}^M + a[1] \mathbf{z}^{M-1} \\ + \dots + a[M-1] \mathbf{z} + a[M]. \quad (8)$$

163 Shifting the index on (5) from n to $n - m$ and multiplying by
164 the parameter $a[m]$ yield

$$a[m] \cdot x[n - m] = a[m] \cdot \sum_{k=1}^M \mathbf{h}_k \mathbf{z}_k^{n-m-1}. \quad (9)$$

165 The (9) can be modified to

$$\sum_{m=0}^M a[m] \cdot x[n - m] = \sum_{k=1}^M \mathbf{h}_k \mathbf{z}_k^{n-M} \left\{ \sum_{m=0}^M a[m] \cdot \mathbf{z}_k^{M-m-1} \right\}. \quad (10)$$

166 The right-hand summation in (10) may be recognized as a
167 polynomial defined by (8), evaluated at each of its roots \mathbf{z}_k
168 yielding the zero result

$$\sum_{m=0}^M a[m] \cdot x[n - m] = 0. \quad (11)$$

169 The equation can be solved for the polynomial coefficients.
170 In the second step, the roots of the polynomial defined by
171 (8) can be calculated. The damping factors and the sinusoidal
172 frequencies may be determined from the roots \mathbf{z}_k .

173 For practical situations, the number of data points N usually
174 exceeds the minimum number needed to fit a model of exponen-
175 tials, i.e., $N > 2M$. In the overdetermined data case, the linear
176 equation (11) must be modified to

$$\sum_{m=0}^M a[m] \cdot x[n - m] = e[n]. \quad (12)$$

177 The estimation problem is based on the minimization of the
178 total squared error

$$E = \sum_{n=M+1}^N |e[n]|^2. \quad (13)$$

179 III. MIN-NORM METHOD

180 The min-norm method involves projection of the signal
181 vector

$$\mathbf{s}_i = \begin{bmatrix} 1 & e^{j\omega_i} & \dots & e^{j(N-1)\omega_i} \end{bmatrix}^T. \quad (14)$$

182 onto the noise subspace.

183 We consider a random sequence x made up of M indepen-
184 dent signals in noise.

$$x = \sum_{i=1}^M A_i s_i + \eta, \quad A_i = |A_i| e^{j\phi_i}. \quad (15)$$

185 If the noise is white, the correlation matrix is

$$\mathbf{R}_x = \sum_{i=1}^M E \{ A_i A_i^* \} s_i s_i^T + \sigma_0^2 \mathbf{I} \quad (16)$$

186 where \mathbf{I} denotes the identity matrix (matrix with 1s on the diag-
187 onal and 0s elsewhere), $*$ denotes the complex conjugate, and

$\{\cdot\}^T$ denotes the matrix transpose operation. $N - M$ smallest
eigenvalues of the correlation matrix of dimension $N > M + 1$ 189
correspond to the noise subspace, and M largest value (all 190
greater than σ_0^2) corresponds to the signal subspace. 191

We define the matrix of eigenvectors 192

$$\mathbf{E}_{\text{noise}} = [\mathbf{e}_{M+1} \quad \mathbf{e}_{M+2} \quad \dots \quad \mathbf{e}_N]. \quad (17)$$

Min-norm method uses one vector \mathbf{d} for frequency estima- 193
tion. This vector, belonging to the noise subspace, has minimum 194
Euclidean norm and its first element is equal to one. These 195
conditions are expressed by the following equations: 196

$$\begin{aligned} \mathbf{d} &= \mathbf{E}_{\text{noise}} \mathbf{E}_{\text{noise}}^{*T} \mathbf{d} \\ \mathbf{d}^{*T} \ell &= 1. \end{aligned} \quad (18)$$

We can express (18) in one equation 197

$$\mathbf{d}^{*T} \ell = (\mathbf{E}_{\text{noise}} \mathbf{E}_{\text{noise}}^{*T} \mathbf{d})^{*T} \ell = \mathbf{d}^{*T} \mathbf{E}_{\text{noise}} \mathbf{E}_{\text{noise}}^{*T} \ell = 1 \quad (19)$$

and form the Lagrangian 198

$$\begin{aligned} L &= \mathbf{d}^{*T} \mathbf{d} + \mu (1 - \mathbf{d}^{*T} \mathbf{E}_{\text{noise}} \mathbf{E}_{\text{noise}}^{*T} \ell) \\ &\quad + \mu^* (1 - \ell^T \mathbf{E}_{\text{noise}} \mathbf{E}_{\text{noise}}^{*T} \mathbf{d}). \end{aligned} \quad (20)$$

The gradient of (20) has the form 199

$$\nabla_{\mathbf{d}^*} L = \mathbf{d} - \mu \mathbf{E}_{\text{noise}} \mathbf{E}_{\text{noise}}^{*T} \ell = 0 \quad (21)$$

where μ is chosen in such way that the first element of the 200
vector is equal to 1. For this purpose, we present $\mathbf{E}_{\text{noise}}$ in 201
the form 202

$$\mathbf{E}_{\text{noise}} = \begin{bmatrix} \mathbf{c}^{*T} \\ \mathbf{E}'_{\text{noise}} \end{bmatrix} \quad (22)$$

where \mathbf{c}^{*T} is the upper row of the matrix. Hence, $\mathbf{c} = \mathbf{E}_{\text{noise}}^{*T} \ell$. 203

From (21) and (22), it results that the first element of the 204
vector \mathbf{d} is equal to $\mu \mathbf{c}^{*T} \mathbf{c}$. Finally, vector \mathbf{d} is equal to 205

$$\mathbf{d} = \frac{1}{\mathbf{c}^{*T} \mathbf{c}} \mathbf{E}_{\text{noise}} \mathbf{c} = \begin{bmatrix} 1 \\ \frac{(\mathbf{E}'_{\text{noise}} \mathbf{c})}{(\mathbf{c}^{*T} \mathbf{c})} \end{bmatrix}. \quad (23)$$

Pseudospectrum, defined with the help of \mathbf{d} , is given as 206

$$\hat{P}(e^{j\omega}) = \frac{1}{|\mathbf{w}^{*T} \mathbf{d}|^2} = \frac{1}{\mathbf{w}^{*T} \mathbf{d} \mathbf{d}^{*T} \mathbf{w}} \quad (24)$$

where \mathbf{w} is defined as 207

$$\mathbf{w} = \begin{bmatrix} 1 & e^{j\omega_i} & \dots & e^{j(N-1)\omega_i} \end{bmatrix}^T. \quad (25)$$

208 IV. EXPERIMENTS WITH SIMULATED WAVEFORMS

209 Several experiments were performed with the signal
 210 waveform obtained from a typical dc-arc-furnace plant of
 211 80-MW nominal power [2]. The supply installation consists of a
 212 medium voltage ac busbar with two parallel thyristor rectifiers
 213 that are fed by a transformer secondary winding with Δ and
 214 Y connection, respectively. The investigated signal is charac-
 215 teristic for dc-arc-furnace installations without compensation.
 216 It consists of a basic harmonic (50 Hz), one higher harmonic
 217 (350 Hz), and one subharmonic (25 Hz) and is additionally
 218 distorted by a 5% random noise. The sampling interval was
 219 1 ms. The signal was obtained by simulation based on real
 220 recordings.

221 The signal was investigated using the Prony and min-norm
 222 methods. Both the methods enable us to detect all the sig-
 223 nal components using 50 samples (Fig. 1). For detecting the
 224 25-Hz component using the Fourier algorithm, approximately
 225 ten times more samples were needed.

226 V. INDUSTRIAL FREQUENCY CONVERTER

227 The investigated drive represents a typical configuration
 228 of industrial drives consisting of a three-phase asynchronous
 229 motor and a power converter composed of a single-phase half-
 230 controlled bridge rectifier and a voltage source converter. The
 231 waveforms of the converter output current under normal condi-
 232 tions (Fig. 2) were investigated using the Prony, the min-norm,
 233 and the FFT methods [11]. The main frequency of the waveform
 234 was 40 Hz.

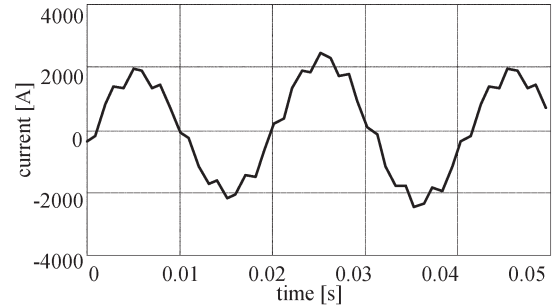
235 Using the Prony and the min-norm methods, the following
 236 harmonics have been detected: fifth, seventh, 17th, 19th, 25th,
 237 35th, and 41st. It is also possible to estimate the frequency of
 238 the fundamental component. Estimation of the main component
 239 frequency enables choosing an appropriate sampling window
 240 for the FFT.

241 VI. OUT-OF-STEP OPERATION OF A 242 SYNCHRONOUS GENERATOR

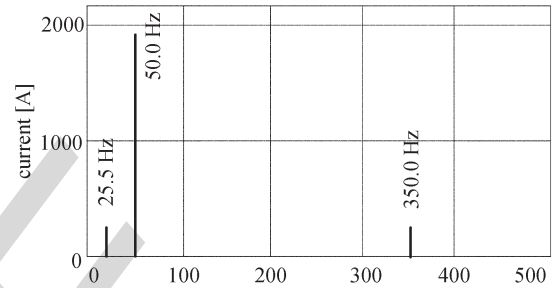
243 If the machine running in parallel with others is disturbed
 244 from its synchronous-state conditions, the rotor-winding and
 245 the stator-winding fluxes rotate with different velocities. The
 246 stator-winding flux generates an electromotive force (EMF)
 247 in the rotor winding whose angular velocity depends on the
 248 rotor slip. The current in the rotor winding caused by the
 249 EMF produces a pulsating magnetomotive force (MMF), which
 250 can be resolved into two “rotating” MMFs of constant and
 251 equal amplitude revolving in opposite directions. These MMFs
 252 are assumed to set up corresponding gap fluxes. The angular
 253 velocities of the fluxes are equal to the angular frequencies of
 254 the alternating components of the rotor-winding current.

$$\omega_f = s \cdot \omega_s \quad \omega_b = -s \cdot \omega_s \quad (26)$$

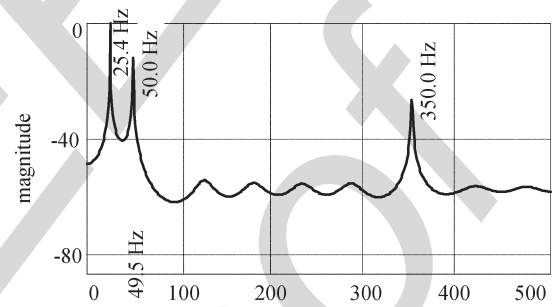
255 where ω_f is the angular velocity of the forward field compo-
 256 nent, ω_b is the angular velocity of the backward field com-
 257 ponent, ω_s is the angular velocity of the rotating stator field,



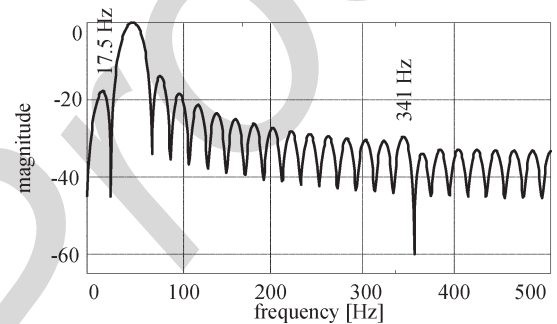
(a)



(b)



(c)



(d)

Fig. 1. Current waveform at the dc-arc-furnace plant investigation results: (a) Prony, $M = 10$, (b) min-norm, (c) FFT, (d) $f_s = 1000$ Hz, $N = 50$, $f_s = 5000$ Hz.

and s is the rotor slip. The angular velocity of the rotor ω_r is 258 described as 259

$$\omega_r = (1 - s)\omega_s. \quad (27)$$

The field components cut the stator conductors at velocities 260 depending on the velocities of the components and the veloc- 261 ity of the rotor. Hence, corresponding EMFs are induced in 262 the stator windings, causing current components to flow. The 263 angular frequencies of the components are ω_s and $(1 - 2s)\omega_s$. 264

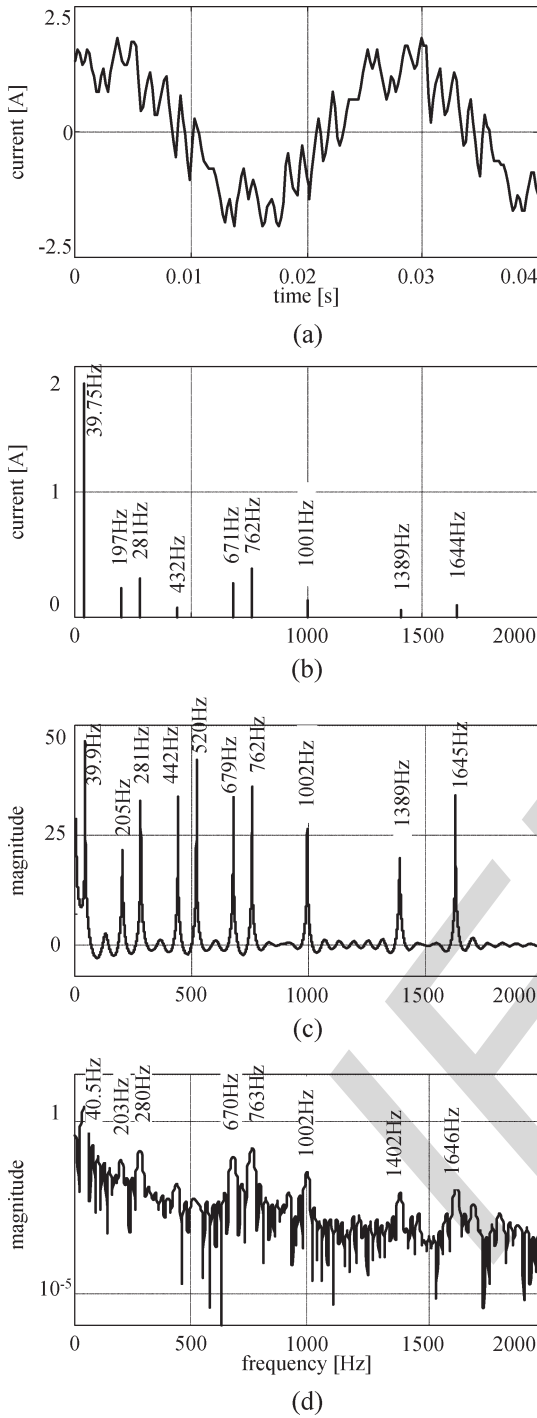


Fig. 2. Current waveform at the output of a real frequency converter investigation results: (a) Prony $N = 200$, $M = 80$, (b) min-norm $N = 100$, (c) FFT $N = 200$, (d) $f_s = 5000$ Hz.

265 Direct current in rotor windings produces MMFs, which set up
 266 corresponding gap fluxes. The fluxes rotate with the angular
 267 velocity ω_r , cut the stator conductors at sleep speed, induce
 268 corresponding UMFs, and cause another component of the
 269 stator currents.

270 A. Simulation of the Fault Operation

271 In the recent years, simulation programs for complex elec-
 272 trical circuits and control systems have been improved essen-

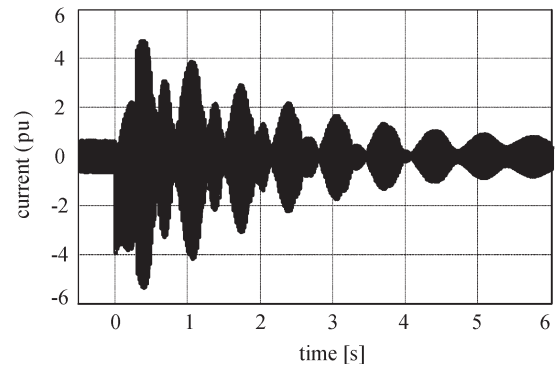


Fig. 3. Current waveform at the generator output. Duration of the fault is 300 ms (pu).

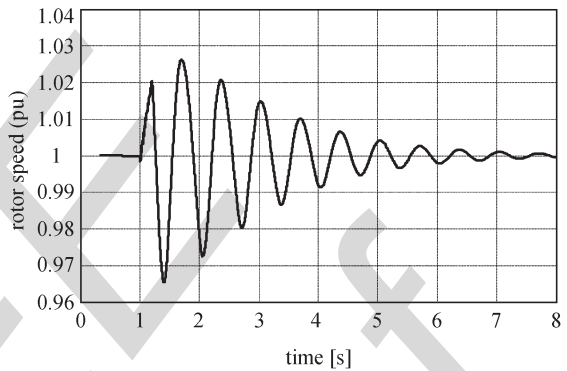


Fig. 4. Rotor speed of the generator during out-of-step operation (pu).

tially. The Electromagnetic Transients Program—Alternative 273
 Transients Program (EMTP—ATP) as a FORTRAN-based and 274
 an MS-DOS/Windows adapted program serves for modeling 275
 complex one- or three-phase networks occurring in drive, con- 276
 trol, and energy systems. 277

In this paper, we show investigation results of the fault 278
 operation of a synchronous generator powered by hydraulic 279
 turbine combined to a proportional-integral-differential (PID) 280
 governor system and an excitation system. The excitation sys- 281
 tem implements IEEE type-1 synchronous machine voltage 282
 regulator combined to an exciter. 283

Generator Data: Salient-pole synchronous generator: 284
 200-MVA nominal power, 13.8-kV nominal voltage, and 285
 50-Hz nominal frequency. 286

- 1) reactances: $X_d = 1.305$, $X'_d = 0.296$, $X''_d = 0.252$, 287
 $X_q = 0.474$, $X''_q = 0.243$ [per unit (pu)]; 288
- 2) block transformer: 210 MVA, 13.8 kV/230 kV, dY , 289
 $R_1 = 0.0027$, $L_1 = 0.08$ (pu); 290
- 3) system: 10 GVA, 230 kV; 291
- 4) sampling frequency: 200 Hz. 292

Under normal steady-state conditions, a three-phase to 293
 ground fault at the transformer output was simulated. The fault 294
 was switched on at $t = 0$. After the fault was cleared, out-of- 295
 step operation conditions occurred. In Fig. 3, the current wave- 296
 form at the generator output for the short-circuit duration of 297
 300 ms is shown; and in Fig. 4, the rotor speed during the fault 298
 is shown. The time–frequency distribution of the waveform 299
 has been calculated by applying the min-norm method and the 300
 window of 40 samples (0.2 s). 301

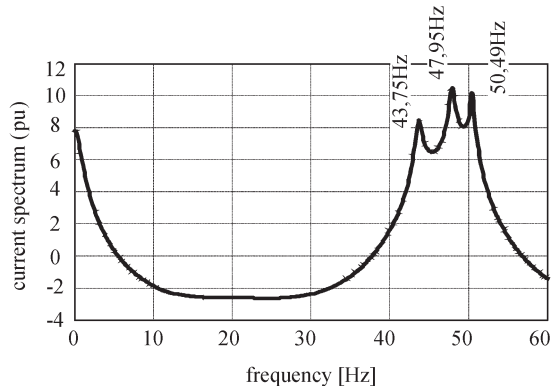


Fig. 5. Stator current spectrum of the signal in Fig. 3 for $t = 2$ s after fault incipience. Detected signal components with frequencies of 43.75, 47.95, and 50.49 Hz.

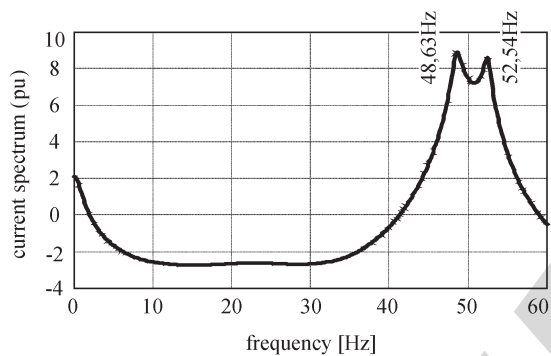


Fig. 6. Stator current spectrum of the signal in Fig. 3 for $t = 4$ s after fault incipience. Detected signal components with frequencies of 48.63 and 52.54 Hz.

In this way, a three-dimensional spectrum has been obtained. In this paper, only some cross sections of the spectrum are shown to demonstrate the high resolution of the method. At the beginning of the asynchronous running, three current frequency components have been detected (Fig. 5). Afterward, the component with the smallest frequency disappeared (Fig. 6). The difference between the frequencies of the two other current components for $t = 4$ sec. is smaller than the value estimated for $t = 2$ sec. The decrease of the frequency differences of the signal components over time confirms the trend toward the retrieval of the generator from the out-of-step state.

VII. CONCLUSION

It has been shown that a high-resolution spectrum-estimation method such as min-norm could be effectively used for parameter estimation of distorted signals. The Prony method could also be applied for estimation of the frequencies of signal components.

The proposed methods were investigated under different conditions and found to be variable and efficient tools for detection of all higher harmonics existing in a signal. They also make possible the estimation of interharmonics. For identification of the asynchronous operation, the frequencies of the current components are estimated. The appearance of additional current frequency components can be used as an indicator of out-of-

step operation of a synchronous machine. The decrease of the frequency differences of the detected current components over time indicates that the generator is leaving the out-of-step state.

REFERENCES

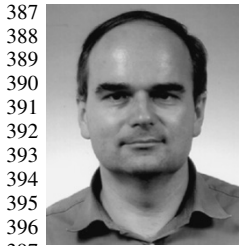
- [1] R. Carbone, D. Menniti, N. Sorrentino, and A. Testa, "Iterative harmonics and interharmonic analysis in multiconverter industrial systems," in *Proc. 8th Int. Conf. Harmonics and Quality Power*, Athens, Greece, Oct. 1998, pp. 432–438.
- [2] A. Bracale, G. Carpinelli, D. Lauria, Z. Leonowicz, T. Lobos, and J. Rezmer, "On some spectrum estimation methods for analysis of non-stationary signals in power systems—Part II: Numerical applications," in *Proc. 11th Int. Conf. Harmonics and Quality Power*, Lake Placid, NY, Sep. 2004, pp. 6–16.
- [3] K.-F. Eichhorn and T. Lobos, "Recursive real-time calculation of basic waveforms of signals," *Proc. Inst. Elect. Eng.*, vol. 138, Pt. C, no. 6, pp. 469–470, Nov. 1991.
- [4] A. Cichocki and T. Lobos, "Artificial neural networks for real-time estimation of basic waveforms of voltages and currents," *IEEE Trans. Power Syst.*, vol. 9, no. 2, pp. 612–618, May 1994.
- [5] Z. Leonowicz, T. Lobos, P. Ruczewski, and J. Szymanda, "Application of higher-order spectra for signal processing in electrical power engineering," *COMPEL—Int. J. Comput. Math. Electr. Electron. Eng.*, vol. 17, no. 5, pp. 602–611, Oct. 1998.
- [6] T. Lobos, T. Kozina, and H. J. Koglin, "Power system harmonics estimation using linear least squares method and SVD," *Proc. Inst. Elect. Eng., Gen. Transm. Distrib.*, vol. 148, no. 6, pp. 567–572, Nov. 2001.
- [7] M. Meunier and F. Brouage, "Fourier transform, wavelets, prony analysis: Tool for harmonics and quality of power," in *Proc. 8th Int. Conf. Harmonics and Quality Power*, Athens, Greece, Oct. 1998, pp. 71–76.
- [8] S. M. Kay, *Modern Spectral Estimation: Theory and Application*. Englewood Cliffs, NJ: Prentice-Hall, 1988, pp. 224–225.
- [9] T. Lobos and J. Rezmer, "Real-time determination of power system frequency," *IEEE Trans. Instrum. Meas.*, vol. 46, no. 4, pp. 877–881, Aug. 1997.
- [10] C. W. Therrien, *Discrete Random Signals and Statistical Signal Processing*. Englewood Cliffs, NJ: Prentice-Hall, 1992, pp. 614–655.
- [11] Z. Leonowicz, T. Lobos, and J. Rezmer, "Advanced spectrum estimation methods for signal analysis in power electronics," *IEEE Trans. Ind. Electron.*, vol. 50, no. 3, pp. 514–519, Jun. 2003.
- [12] T. Lobos, Z. Leonowicz, and J. Rezmer, "Harmonics and interharmonics estimation using advanced signal processing methods," in *Proc. 9th Int. Conf. Harmonics and Quality Power*, Orlando, FL, Oct. 2000, vol. 1, pp. 335–340.



Tadeusz Lobos received the M.Sc., Ph.D., and Dr.Sc. (Habilitation Doctorate) degrees from the Wrocław University of Technology, Wrocław, Poland, in 1960, 1967, and 1975, respectively, all in electrical engineering.

Since 1960, he has been with the Department of Electrical Engineering, Wrocław University of Technology, where he became a Full Professor in 1989. From 1982 to 1986, he worked at the University of Erlangen-Nuremberg, Germany. His current research interests include transients in power systems, control and protection, and especially application of neural networks and signal processing methods in power systems.

Dr. Lobos was awarded a Research Fellowship in 1976 by the Alexander von Humboldt Foundation, Germany. He spent this fellowship at the Technical University of Darmstadt, Darmstadt, Germany. He received the Humboldt Research Award, Germany, in 1998.



Zbigniew Leonowicz (M'03) received the M.Sc. and Ph.D. degrees from Wroclaw University of Technology, Wroclaw, Poland, in 1997 and 2001, respectively, all in electrical engineering.

From 2003 to 2004, he worked as a Research Scientist at the Brain Science Institute, Institute of Physical and Chemical Research (RIKEN), Saitama, Japan. Since 1997, he has been with the Department of Electrical Engineering, Wroclaw University of Technology. His current research interests include modern digital signal-processing methods applied to

398 power-system analysis.

399 Dr. Leonowicz was awarded an Advanced Fellowship by the North Atlantic
400 Treaty Organization (NATO) in 2001. He spent this fellowship at the Technical
401 University of Dresden, Germany.



Peter Schegner (M'00) received the M.Sc. degree 409
in electrical power engineering from Darmstadt Uni- 410
versity of Technology, Darmstadt, Germany, in 1982 411
and the Ph.D. degree from Saarland University, 412
Saarland, Germany, in 1989 with a thesis on the 413
earth-fault distance protection. 414

In 1982, he worked as a System Engineer in the 415
field of power-system control and became a member 416
of the Scientific Staff at Saarland University. From 417
1989 until 1995, he worked as the Head of the 418
Development Department of Protection Systems at 419

the AEG, Frankfurt AM, Germany. In 1995, he became a Full Professor 420 **AQ2**
and the Head of the Institute of Electrical Power Systems and High-Voltage 421
Engineering, Dresden University of Technology, Dresden, Germany. 422



Jacek Rezmer received the M.Sc. and Ph.D. degrees from Wroclaw University of Technology, Wroclaw, Poland, in 1987 and 1995, respectively, all in electrical engineering.

His primary professional interests lie in the new signal-processing methods for electric power-system analysis.

LEEEF
Proof

AUTHOR QUERIES

AUTHOR PLEASE ANSWER ALL QUERIES

AQ1 = Data on the first footnote is derived from vitae. Please check if correct.

AQ2 = Please provide the expanded form of the acronym "AEG."

Note: Photo of P. Schegner is pixelated/blurred.

END OF ALL QUERIES

IEEE
Proof